(57) Olabisi, O.; Robeson, L. M.; Shaw, M. T. "Polymer–Polymer Miscibility"; Academic Press: New York, 1979.
(58) Gregonis, D. E.; Hsu, R.; Buerger, D. E.; Smith, L. M.; Andrade, J. D. In "Macromolecular Solutions"; Seymour, R. B., Stahl, G. A., Eds.; Pergamon Press: New York, 1982; pp 120–133.
(59) Ratner, B. D.; Weathersby, P. K.; Hoffman, A. S.; Kelly, M. A.; Scharpen, L. H. *J. Appl. Polym. Sci.* 1978, *22*, 643.

X-ray Evidence of an α-Helical Coiled Coil in Poly(γ-dodecyl L-glutamate)

Junji Watanabe* and Hirobumi Ono

Department of Polymer Chemistry, Tokyo Institute of Technology, Ookayama, Meguro-ku, Tokyo, 152 Japan. *Received June 19, 1985*

ABSTRACT: The X-ray diagram of an as-cast film of α-helical poly(γ-dodecyl L-glutamate) displays several striking features: a strong 5.14-Å meridional reflection and a near-equatorial layer line located $^1/_{90}$ Å^{-1} from the equator. These features cannot be accounted for by a simple α-helical conformation but require an α-helical coiled coil. Moreover, the two-chain hexagonal unit net and the assignment of the near-equatorial line to the second layer ($l = 2$) can only be explained by a two-strand structure. These data provide the first X-ray evidence for a coiled-coil structure in a homopolypeptide in which the structure is not stabilized by amphipathic interactions due to a particular sequence of repeating units. From the intensity distribution of the equatorial reflections the radius of the coiled coil is about 5.6 Å. A possible model is described in which the coiled coil consists of two close-packed α-helices with the side chains mainly on the outer surface.

Introduction

The α-helical model accounts satisfactorily for the X-ray diffraction pattern of synthetic polypeptides in the α-form. However, in its simplest form it does not account for the 5.15-Å meridional reflection obtained from the keratin–myosin–epidermin–fibrinogen groups of fibrous α-proteins.[1] Crick[2] and Pauling and Corey[3] independently suggested that this reflection could arise if the axes of the α-helices were distorted to form a long-pitch helix. The resulting conformation was termed a coiled coil.

Pauling and Corey[3] proposed that the distortion arises from the formation of hydrogen bonds of slightly different lengths due to the repeating sequence. A more plausible explanation was offered by Crick,[4] who suggested that supercoiling of two or three α-helices might be stabilized by a regular interlocking of the side chains. Figure 1a represents a radial projection of two α-helices in which the side chains (considered as "knobs") are represented as open and filled circles for the two helices. Crick[4] pointed out that "knob into hole" packing could be achieved over the entire chain length if the chains coiled about each other, as shown in Figure 1b, with the axes of the helices mutually inclined at an appropriate angle α. He derived the structure factor for the following model. The curved α-helix is termed the minor α-helix, and r_j' is the distance of the jth atom from the axis of the minor helix. The more gradual helix traced by the axis of the minor α-helix is termed the major helix. It has radius r_0 and repeat distance C in the z direction. The major helix makes N_0 turns and the minor helix N_1 turns in its own frame, and there are M equally spaced jth atoms in that repeat distance. The values of C, N_0, N_1, and M are 186 Å, 1, 36, and 128, respectively. Denoting the cylindrical coordinates in reciprocal space as R, Ψ, and Z, one may write the structure factor as

$$F(R,\Psi,Z) = F(R,\Psi,l/C) = \sum_p\sum_q\sum_s\sum_j J_p(2\pi R r_0) f_j J_q(2\pi R r_j') J_s\{2\pi(l/C) r_j' \sin\alpha\} \times \exp\{i[p(\pi/2 - \psi_j + \Psi) + q(\pi/2 + \psi_j - \Psi) + s\pi + 2\pi l z_j/C]\} \quad (1)$$

Here f_j is the scattering factor of the jth atom, $J_n(X)$ is the nth-order Bessel function of X, and r_j', ψ_j, and z_j are cylindrical coordinates in real space. The structure factor is nonzero only on layer lines l that satisfy the condition

$$p + 35q + 36s = l + 126m \quad (2)$$

where p, q, s, and m can take integer values. These relations explain the meridional reflection at about 5.15 Å and the strong near-equatorial streak seen in the X-ray patterns of fibrous proteins,[6-9] while neither of these features is expected for straight α-helices.

Crick also suggested[4] that the primary structure stabilizes supercoiling. Elucidation[10-15] of the primary structure of tropomyosin has clarified this relationship. In particular, sequence analysis[10-13] of the tropomyosin chain from rabbit skeletal muscle showed that hydrophobic residues occur at intervals of seven residues. This sequence produces a densely packed hydrophobic region between the two helices, while the longer charged groups (such as arginine, lysine, and glutamic acid) are located on the surface of the coiled coil and are responsible for the solubility and interaction properties. In contrast, Parry and Suzuki[16] concluded from potential energy calculations of poly(L-alanine) that coiled coils are generally more stable than the corresponding single helices. This suggests that no particular repeating sequence of residues is necessary to stabilize the coiled coil. However, there has been no report of synthetic polypeptides in a coiled-coil conformation. They suggested that this may be due to large voids in the coiled-coil structure which can only be filled with a suitable solvent. Some features of the X-ray diffraction pattern expected for coiled coils have been observed for the concentrated phase of poly(γ-benzyl L-glutamate) in *N*,*N*-dimethylformamide.[9,17,18] However, the α-helices in this "complex phase" are straight, and the long-period helix is due to the regular arrangement of the terminal benzyl groups.[17,18] Watanabe et al.[19] confirmed that the benzene rings are cooperatively stacked both in the "complex phase" and in the dried film. This appears to be a stable arrangement, since many other examples of such a face-to-face stacking of benzene rings have been reported.[20-23]

This paper presents the first X-ray evidence for coiled coils in a synthetic homopolypeptide, poly(γ-dodecyl L-glutamate) (PDoDLG), having the following repeating unit

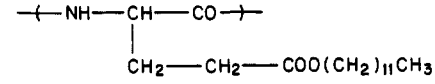

0024-9297/86/2219-1079$01.50/0

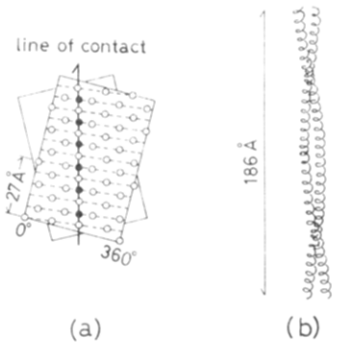

Figure 1. (a) Pattern formed by side chains along the line of contact of two α-helices where the side chains of one helix are represented by open circles and ones of the other by filled circles. (b) Model of two-strand coiled coil.

While the X-ray pattern is poor in some respects, it does exhibit several features expected for a coiled-coil conformation. It is unlikely that the flexible side chains would exhibit the type of regular stacking found in poly(γ-benzyl L-glutamate), so these features must be attributed to supercoiling.

Experimental Section

Materials. Poly(γ-dodecyl L-glutamate) was synthesized by the conventional NCA method. The structure was confirmed by NMR spectra. Its intrinsic viscosity, as determined in dichloroacetic acid by a Ubbelohde viscometer, was 0.34 dL/g. This is approximately half the value, 0.62 dL/g, observed for the same polymer prepared from poly(γ-methyl L-glutamate) by ester interchange and having a degree of polymerization of 700, so we assume that the degree of polymerization of the present polymer is approximately 350.

Preparation of Films. Films were prepared by casting from chloroform solutions. The density of the film, as determined at room temperature by flotation using aqueous KBr solutions, was 1.01 g/mL. The presence of amide structures I, II, and V was indicated by IR bands at 1650, 1546, and 615 cm^{-1}, respectively, which indicates that the main chain has an α-helical conformation. Further confirmation was provided by the value, $b_0 = -600$, determined from an ORD measurement of the chloroform solution.

X-ray Measurements. Uniaxially oriented films were prepared by stroking concentrated chloroform solutions. The films so prepared were annealed at 40 °C in an atmosphere of chloroform vapor and then dried under vacuum. X-ray photographs were taken by using flat-plate or cylindrical cameras. Silicon crystals coated on the specimens were used for calibration. Relative intensities were determined by a microphotometer using the multiple-film method. These were corrected for Lorentz and polarization effects and for multiplicity of reflections.

Results and Discussion

A. Description of the Diffraction Pattern. Figure 2a illustrates an X-ray photograph taken with the beam parallel to the film surface and perpendicular to the orientation direction. As indicated in Table I, the seven equatorial reflections can be indexed to a two-dimensional hexagonal net having $a = b = 27.6$ Å. The calculated density with two α-helices in the unit net is 1.00 g/mL, which stands in good agreement with the measured density. There are few reflections on the other layer lines, which indicates a packing disorder along the chain axis. This may arise from rotational and translational disorder. Despite this lack of detail, the pattern exhibits some predominant features, which are listed in Table I. The most striking of these is a near-equatorial layer line about $^1/_{90}$ $Å^{-1}$ from the equator. This can be seen in the photograph in Figure 2a and is illustrated for better clarity in the diagram shown in Figure 2c. Its maximum intensity occurs at approximately 13 Å, since an intense reflection appears above the 110 reflection at 13.8 Å, and a weak one above the 200 reflection at 12 Å. A second prominant feature is the meridional reflection at 5.14 Å. The tilted diffraction pattern shown in Figure 2b shows another meridional reflection at 1.50 Å. These features cannot be explained by a structure of straight helices but require the two-strand coiled coil, which forms the basis of Crick's model.

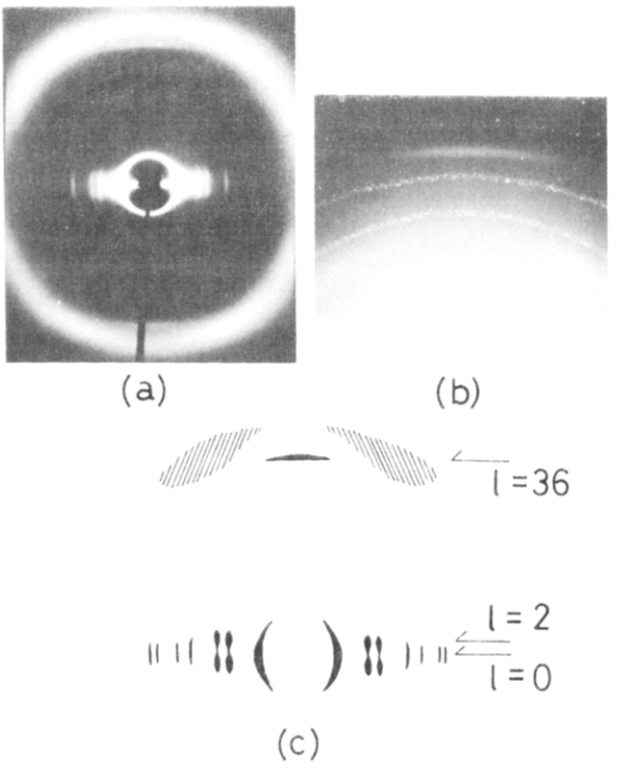

Figure 2. (a) X-ray diagram obtained from oriented films of poly(γ-dodecyl L-glutamate). The X-ray beam was irradiated perpendicular to the orientation direction and parallel to the film surface. (b) As in (a), but with the orientation axis tilted so as to bring out the 1.5-Å meridional reflection. (c) Schematic representation of diagram of (a).

Table I
X-ray Data of Poly(γ-dodecyl L-glutamate)

d_{obsd}, Å	d_{calcd},[a] Å	hkl[a]	I_{obsd}	$I_{obsd}^{1/2}$
23.9	23.90	100	100	10
13.8	13.80	110	4.28	2.07
12.0	11.95	200	5.26	2.29
9.05	9.03	210	3.81	1.95
7.98	7.97	300	2.90	1.70
6.91	6.90	220	~1.6	~1.3
6.63	6.63	310	~1.6	~1.3

d, Å	type of reflection	l[b]
~90	near equatorial	2
5.14	meridional	36
1.50	meridional	126

[a] Based on the hexagonal unit cell with $a = 27.6$ Å. [b] Based on the α-helical coiled-coil conformation (see text).

B. Equatorial Layer Line. It is significant that evidence for two chains in the unit net appears in the equatorial reflections. This means that the two chains are not crystallographically equivalent when viewed in projection along the axis. This observation can be explained by two models: (1) The unit net contains two chains which would be crystallographically equivalent except that their chain directions are antiparallel. (2) The two chains in the unit net are closely associated. The first model can be eliminated, since we have demonstrated that two antiparallel chains are indistinguishable in axial projection.[22,24]

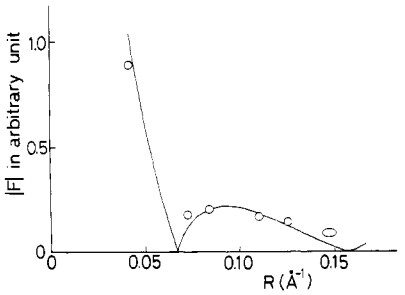

Figure 3. Observed amplitudes (denoted by open circles) of equatorial reflections of poly(γ-dodecyl L-glutamate). The solid curve indicates the calculated amplitude from the coiled coil with the radius of major helix of 5.6 Å (see text).

Table II
Possible Set of Atomic Parameters of Poly(L-glutamate)[a]

atom	r', Å	Ψ, deg	z, Å	B, Å²
		Main Chain		
N	1.55	0	0	2
C_α	2.28	28.7	0.87	2
C′	1.64	54.6	1.96	2
=O	1.86	46.8	3.16	2
		Side Chain		
C_β	3.22	47.3	0.04	5
C_γ	4.14	53.1	0.92	10
C_δ	5.58	59.5	0.09	15
=O	5.45	61.5	−1.13	20
—O—	6.73	61.1	0.79	30
C_ϵ	7.86	64.3	−0.02	40

[a] r', ψ and z are cylindrical coordinates; B is the temperature factor.

This model has the further defect that two straight α-helical chains could not be packed into a simple hexagonal net. The two chains must therefore be closely associated, and this can most easily occur by assembly into a coiled coil.

C. Structure Amplitudes of the Equatorial Reflections. Table I lists the observed structure amplitudes obtained by photometering along the middle of the equatorial line. It is possible that the intensities of the 110 and 200 reflections may have been overestimated due to overlap with the near-equatorial layer line. Despite this possibility, we can conclude that the 110 reflection is the weaker of the two and that the intensities of both these reflections are weaker than the intensity of the 100 reflection. A plot of the observed structure amplitudes appearing in Figure 3 suggests that the Fourier transform falls to zero around $R = 0.06$ Å^{-1} (inside the 110 reflection). This distribution is notably different from that plotted in Figure 4 for the poly(L-glutamates) having hexagonally packed, straight α-helices, such as the methyl, hexyl, and octyl derivatives.[25] A common curve can be obtained by arbitrary scaling, and this decreases monotonically at least until $R = 0.2$ Å^{-1}.

We begin by comparing the observed and calculated structure amplitudes for the latter class of polymer. For straight α-helices, the equatorial structure amplitudes can be calculated[26] from

$$F(R,\Psi,0) = \sum_j f_j J_0(2\pi R r_j') \qquad (3)$$

The main-chain coordinates of the α-helix are given in Table II, but some assumption must be made concerning the side-chain conformations. Fortunately Figure 4 simplifies this problem, since the distribution of structure amplitudes is the same for all three polymers. This indicates that the long side groups do not assume a fixed conformation, have high temperature factors, and make

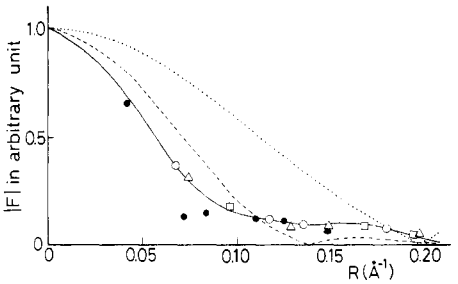

Figure 4. Observed amplitudes of equatorial reflections of PMLG (□), PHLG (△), and POLG (○). Three curves indicate the amplitudes calculated on the basis of the different models: dotted curve, amplitudes from the main-chain atoms and the β-carbon atom; dashed and solid curves, amplitudes from the main-chain atoms and side-chain atoms through C_ϵ in two different conformations (see text). For reference, the observed amplitudes of PDoDLG in Figure 3 are also plotted by filled circles.

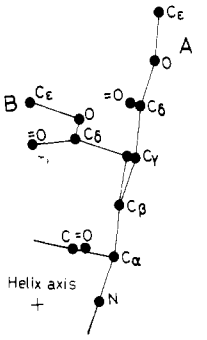

Figure 5. Possible conformations of the side chain (projection along the helix axis): (A) the extended conformation; (B) the conformation in which the side chain is wrapped closely about the main-chain helix.

no significant contribution to the structure amplitude. However, when we take into account only the main-chain and β-carbon atoms, we obtain the calculated structure amplitudes represented by the dotted curve in Figure 4. The agreement between these calculated and observed structure amplitudes is poor. Side-chain atoms through C_ϵ were then included by using the atomic coordinates listed in Table II and illustrated in model A of Figure 5. This model leads to the solid curve in Figure 4, which is in good agreement with observation. Model B in Figure 5, in which the side chain is wrapped closely about the main chain,[27] leads to poorer agreement, as illustrated by the dashed curve in Figure 4. It should be noted that dynamic mechanical measurements indicate the side chains are liquid-like at room temperature. Their glass transition temperatures are[25] 0 °C for PMLG, −35 °C for PHLG, and −37 °C for POLG. Hence, the nearly extended conformation for the first five atoms only represents an averaged conformation.

Returning to PDoDLG, no conformation of the side-chain atoms through C_ϵ could be found to represent the observed structure amplitudes by using a straight α-helical model; the amplitudes calculated for all these models fell between the solid and dashed curves in Figure 4. The unusual appearance of the observed amplitudes may be due to the coiled-coil conformation. The relation for the equatorial structural amplitudes determined from eq 1 and 2 is

$$F(R,\Psi,0) = F_0(2\pi R r_0)\sum_j f_j F_0(2\pi R r_j') \qquad (4)$$

Here the higher order Bessel functions have been neglected, as in eq 3. This equation is very useful since it does not require the coordinates of the distorted α-helices,

but only the radius, r_0, of the major helix in the first Bessel function and the undistorted α-helix coordinates of one residue in the second.[4,28] We assume that the second contribution can be approximated by the common structure amplitude observed for the above three polymers. Taking r_0 = 5.6 Å, we obtain the calculated solid curve shown in Figure 3, which gives a reasonable representation of the observed structure amplitudes of PDoDLG. Moreover, the value of r_0 chosen is near the values obtained for α-protein coiled coils.[7,8]

D. Near-Equatorial Layer Line. According to Crick's treatment, this layer line is related to the pitch and symmetry of the major helix, and its index indicates the number of strands in the structure. Two minor helices are related by a strict dyad along the helix axis, so only every second layer line appears. Three helices form a triad, and in this case only every third layer line is allowed, as can be deduced from the phase term in eq 1. Since the pitch of the major helix is 186 Å, the first near-equatorial layer line at $^1/_{90}$ Å^{-1} can be attributed to l = 2 (186 Å = 93 Å × 2), leading to the conclusion that there are two chains in the structure. This confirms the conclusion deduced above from the size of the unit net.

For the coiled coil, the structure amplitude of the near-equatorial layer line can be written from eq 1 as

$$F(R,\Psi,l/C) = \sum_p J_p(2\pi Rr_0)\sum_j f_j J_0(2\pi Rr_j')J_0\{2\pi(l/C)r_j' \times \sin\alpha\} \exp\{i[p(\pi/2 - \psi_j + \Psi) + 2\pi l z_j/C]\} \quad (5)$$

with the condition $p = l$. For small values of l, $J_0\{2\pi(l/C)r_j \times \sin\alpha\}$ is approximately unity. Moreover, $\sum_j f_j J_0(2\pi Rr_j')$ is a slowly varying function of R, as observed above. Hence, the position of the first maximum will be determined by $J_p(2\pi Rr_0)$.[4] Inserting $l = p = 2$ and r_0 = 5.6 Å and adopting the observed structure amplitude (the solid curve of Figure 4) for $\sum_j f_j J_0(2\pi Rr_j')$, we find that the spacing of the maximum is around $^1/_{15}$ Å^{-1}. Thus one can expect to find some reflections near 15 Å. This conclusion is in qualitative accord with the position of the second layer line above the 110 and 200 reflections, which have spacings of 13.8 and 12.0 Å, respectively.

E. 5.14-Å Reflection on l = 36. Equations 1 and 2 indicate that l for a meridional reflection must be a multiple of 18. The intensity observed in the meridional region of the 5.14-Å layer line is indexed as l = 36. Hence, the spacings of the meridional reflections are submultiples of $^{18}/_{186}$ Å^{-1} = $^1/_{10.3}$ Å^{-1}. These arise from the fact that every 10.3 Å the coiled-coil conformation brings every seventh inward-pointing residue into an equivalent position along the major axis, as indicated in Figure 1a. These reflections are expected to be more intense for lower s values.[4] This predicts that the first intense meridional reflection should arise at 5.15 Å (l = 36) with s = 1, just as observed. Similarly, an intense meridional reflection is expected at 1.48 Å (l = 126) with s = 0. In fact, the corresponding meridional reflection appears at 1.50 Å, which corresponds to the repeat length of the α-helix. Crick[4] has suggested that the 1.5-Å reflection arises from the precise repeat of the main chain, while the 5.14-Å reflection is due to the less regular repeat of the side chains or the first atoms of the side chains. The expected 1.48-Å reflection may have been unobservable due to overlap with the stronger 1.50-Å reflection.

Concluding Remarks

The most notable features in the X-ray diagram of poly(γ-dodecyl L-glutamate) are a 5.14-Å meridional reflection and a near-equatorial line around 90 Å. These features can be accounted for by an α-helical coiled-coil conformation. The radius of the major helix, as determined from the amplitudes of the equatorial reflections, is 5.6 Å. Two additional observations, the two-chain hexagonal unit net and the fact that the first off-equatorial line corresponds to l = 2, require two chains in the structure.

We have previously found[25] that the coiled-coil phase (phase B) occurs between phase A having a crystalline arrangement of the side chains and liquid crystal phase C. The transition from one phase to another is first order and occurs at a definite temperature. For example, the A–B transition occurs at 15 °C, and B–C at 50 °C. The fact that the side chains can crystallize independent of the main-chain conformation indicates that at least the outer portions of the side chains have considerable configurational freedom. In phase B the side chains should be in the liquid state and might resemble a liquid paraffin. In the liquid crystal phase C each α-helix is the kinetic unit. In a previous paper,[25] a similar phase behavior was observed for polymers having side chains longer than decyl, and this was attributed to the liquid nature of the long side chains.[29]

We can imagine that the long side chains act as a solvent in filling the voids produced by forming the coiled coil. In fact, the radius of the major helix is the same order of magnitude as that (r = 6 Å) for the single α-helix of poly(γ-methyl L-glutamate), which indicates that the longer side chains of the coiled-coil structure must be on the surface. Only the portion of the side chain near the main chain contributes to the "knob into hole" packing, and the remainder extends out on the surface of the coiled coil. This can be understood if we note that the "knob into hole" packing of the two chains only occurs in the narrow region along the line of contact, as illustrated in Figure 1a.

Although a particular amino acid sequence may stabilize the coiled-coil conformation, the present study indicates that this is not a necessary condition, as suggested by Parry and Suzuki.[16]

Registry No. PDoDGL, 29439-75-6; PDoDGl (SRU), 51949-42-9.

References and Notes

(1) Fraser, R. D. B.; MacRae, T. P. "Conformation in Fibrous Proteins"; Academic Press: New York, 1973.
(2) Crick, F. H. C. *Nature (London)* **1952**, *170*, 882.
(3) Pauling, L.; Corey, R. B. *Nature (London)* **1953**, *171*, 59.
(4) Crick, F. H. C. *Acta Crystallogr.* **1953**, *6*, 685, 689.
(5) Lang, A. R. *Acta Crystallogr.* **1956**, *9*, 436.
(6) Fraser, R. D. B.; MacRae, T. P. *J. Mol. Biol.* **1961**, *3*, 640.
(7) Cohen, C.; Holmes, K. C. *J. Mol. Biol.* **1963**, *6*, 423.
(8) Fraser, R. D. B.; MacRae, T. P.; Miller, A. *J. Mol. Biol.* **1965**, *14*, 432.
(9) Elliott, A.; Lowy, J.; Parry, D. A. D.; Vibert, P. J. *Nature (London)* **1968**, *218*, 656.
(10) Sodek, J.; Hodges, R. S.; Smillie, L. B.; Jurasek, L. *Proc. Natl. Acad. Sci. U.S.A.* **1972**, *69*, 3800.
(11) Hodges, R. S.; Sodek, J.; Smillie, L. B.; Jurasek, L. *Cold Spring Harbor Symp. Quant. Biol.* **1972**, *37*, 299.
(12) Maclachlan, A. D.; Stewart, M. *J. Mol. Biol.* **1975**, *98*, 293.
(13) Stone, D.; Smillie, L. B. *J. Biol. Chem.* **1978**, *253*, 1137.
(14) Parry, D. A. D. *J. Mol. Biol.* **1981**, *153*, 459.
(15) Capony, J. P.; Elzinga, M. *Biophys. J.* **1981**, *33*, 148.
(16) Parry, D. A. D.; Suzuki, E. *Biopolymers* **1969**, *7*, 189, 199.
(17) Parry, D. A. D.; Elliott, A. *J. Mol. Biol.* **1967**, *25*, 1.
(18) Squire, J. M.; Elliott, A. *Mol. Cryst. Liq. Cryst.* **1969**, *7*, 457.
(19) Watanabe, J.; Kishida, T.; Uematsu, I., to be published.
(20) Watanabe, J.; Imai, K.; Kosaka, K.; Abe, A.; Uematsu, I. *Polym. J. (Tokyo)* **1981**, *13*, 603.
(21) Mitsui, Y.; Iitaka, Y.; Tsuboi, M. *J. Mol. Biol.* **1967**, *24*, 15.
(22) Squire, J. M.; Elliott, A. *J. Mol. Biol.* **1972**, *65*, 291.
(23) Watanabe, J.; Uematsu, I. *Polymer* **1984**, *25*, 1711.
(24) Watanabe, J.; Imai, K.; Gehani, R.; Uematsu, I. *J. Polym. Sci., Polym. Phys. Ed.* **1981**, *19*, 653.
(25) Watanabe, J.; Ono, H.; Uematsu, I.; Abe, A. *Macromolecules* **1985**, *18*, 2141.

(26) Cochran, W.; Crick, F. H. C.; Vand, V. *Acta Crystallogr.* **1952**, *5*, 581.
(27) Yan, J. F.; Vanderkooi, G.; Scheraga, H. A. *J. Chem. Phys.* **1968**, *49*, 2713. The energy calculation for isolated poly(L-glutamates) in this paper indicates that this conformation of the side chain is the one of lowest energy.
(28) Fraser, R. D. B.; MacRae, T. P.; Miller, A. *Acta Crystallogr.* **1964**, *17*, 813.
(29) Watanabe, J.; Fukuda, Y.; Gehani, R.; Uematsu, I. *Macromolecules* **1984**, *17*, 1004.

Dynamic Light Scattering on Semidilute Solutions of High Molecular Weight Polystyrene in Ethyl Acetate

Wyn Brown

Institute of Physical Chemistry, University of Uppsala, S-751 21 Uppsala, Sweden.
Received May 6, 1985

ABSTRACT: Data obtained with quasi-elastic light scattering and gradient diffusion measurements on semidilute solutions in the $qR_g > 1$ range are presented for the polystyrene/ethyl acetate (marginal solvent) system. The time correlation function was analyzed by the method of cumulants and also fit by using one-, two-, and three-exponential expressions. Optimal fit was consistent with two exponents. The fast and slow components were both found to be q^2-dependent and also independent of molecular weight. It is concluded that two cooperative modes are required to describe a heterogeneous semidilute solution structure for polymers of high molecular weight. This agrees with the model of Brochard for poor solvent systems in the high-q region. The slower mode has a correlation length of the magnitude of the radius of the coil. Comparison with data in a good solvent (THF) and a Θ solvent (cyclopentane) show that D_f and D_s are strongly solvent-dependent as functions of concentration. This contrasts with the solvent-independent universal length recently demonstrated for the static parameter. The relative intensity contribution of D_f increased slowly with concentration as in the Θ system, in contrast to a rapid increase in a good solvent.

Introduction

There is currently a degree of confusion prevailing in the literature concerning the interrelationship between static and dynamic aspects of semidilute solution behavior and the way in which marginal solvents fit into the picture.

A feature that has been noted in quasi-elastic light scattering (QELS) studies is the systematic trend in the variance, μ_2/Γ^2, as measured by the cumulants method,[1] with increasing concentration.[2-6] The cumulants method, however, permits no further progress in understanding the possible causes that underly this behavior. Finite values of the line width in dilute solution reflect polydispersity, whereas in semidilute solutions a reasonable explanation for the relatively large variance is the presence of a small number of discrete exponentials describing complementary modes.[2,3] Such an assumption does not exclude the possibility of a more complex distribution of exponentials but is in line with current theory[7-10] for poor solvent systems and also finds support in elastic neutron and light scattering results[12] for polystyrene (PS) as semidilute concentrations in both good and poor solvents. If the possible validity of this view is conceded, a variety of approaches exist for analyzing the time correlation function and have been applied by various groups. Thus Chu and co-workers[2,3,11] used the histogram method to analyze $S(q,t)$ data for PS in poor solvent systems and interpreted the results in terms of two contributing modes of similar time scale. Other groups[5,13] have used CONTIN, a Fortran program introduced by Provencher.[14,15] The method of discrete multiexponentials has been used by others.[6,16-20] There will inevitably exist a measure of disagreement on the relative virtues of the various methods, and an objective appraisal of the particular advantages of the approaches is at present lacking. We use the method of discrete multiexponentials, which, although requiring an assumption of the number of participating relaxation processes, has particular relevance here. Recent reports described QELS measurements on the same polystyrene fractions at semidilute concentrations in both a good solvent (THF)[19] and in a Θ solvent (cyclopentane)[20] in the gel region. In the good solvent system the data were found to be consistent with the presence of fast and slow components differing in relaxation time by a factor of typically 3–5, whereas only a single gel mode was anticipated from theory.[7,8] A method of analysis having high resolution was thus essential. By the use of both computer-simulated experiments and measurements on mixtures of monodisperse fractions, it was established that the presently used method gives superior resolution when the relaxation times approach each other. It was suggested[19,20] that the modes separated, both of which are molecular weight independent, must reflect a fundamental heterogeneity of the semidilute solution structure. The slow mode was viewed in these papers as distinct from that which has been the subject of recent debate.[5,13,21-24] The latter is frequently orders of magnitude slower than the fast mode and may be separated experimentally by varying the sampling time. There is evidence[13,21,24] suggesting that this slow mode derives from the dynamics of clusters of chains.

Earlier reports[25-28] in which data interpretation was based on the assumption that the dynamic structure factor is a single exponential will need reappraisal if the gel mode is in fact a composite quantity in semidilute solutions. For example, the power law characterizing the concentration dependence will be strongly influenced by the change in the relative weighting between the modes over a given concentration interval.

The present paper has two aims: one is to further examine the nonuniform nature of semidilute solution structure, and the other is to elucidate the influence of solvent quality on the behavior of the transient gel.

Dynamic behavior in so-called "marginal" solvents, i.e., those in which there are only weak excluded-volume interactions, is still controversial. A QELS study[6] on PS of lower molecular weight, in solvents including ethyl acetate, established that the time correlation functions are strongly nonexponential and could be fit with a bimodal function. However, the interpretation to be placed on these com-

0024-9297/86/2219-1083$01.50/0